Geophysical Research Letters

RESEARCH LETTER
10.1029/2022GL100646

Baroclinic Ocean Response to Climate Forcing Regulates Decadal Variability of Ice-Shelf Melting in the Amundsen Sea

Alessandro Silvano[1], Paul R. Holland[2], Kaitlin A. Naughten[2], Oana Dragomir[1], Pierre Dutrieux[2], Adrian Jenkins[3], Yidongfang Si[4], Andrew L. Stewart[4], Beatriz Peña Molino[5,6,7], Gregor W. Janzing[2,8,9], Tiago S. Dotto[10], and Alberto C. Naveira Garabato[1]

[1]Ocean and Earth Science, University of Southampton, Southampton, UK, [2]British Antarctic Survey, Cambridge, UK, [3]Department of Geography and Environmental Sciences, Northumbria University, Newcastle upon Tyne, UK, [4]Department of Atmospheric and Oceanic Sciences, University of California, Los Angeles, CA, USA, [5]CSIRO Oceans & Atmosphere, Hobart, TAS, Australia, [6]Centre for Southern Hemisphere Oceans Research, Hobart, TAS, Australia, [7]Australian Antarctic Program Partnership, University of Tasmania, Hobart, TAS, Australia, [8]Institute for Marine and Atmospheric Research, Utrecht University, Utrecht, The Netherlands, [9]Department of Earth Sciences, Utrecht University, Utrecht, The Netherlands, [10]Centre for Ocean and Atmospheric Sciences, School of Environmental Sciences, University of East Anglia, Norwich, UK

Abstract Warm ocean waters drive rapid ice-shelf melting in the Amundsen Sea. The ocean heat transport toward the ice shelves is associated with the Amundsen Undercurrent, a near-bottom current that flows eastward along the shelf break and transports warm waters onto the continental shelf via troughs. Here we use a regional ice-ocean model to show that, on decadal time scales, the undercurrent's variability is baroclinic (depth-dependent). Decadal ocean surface cooling in the tropical Pacific results in cyclonic wind anomalies over the Amundsen Sea. These wind anomalies drive a westward perturbation of the shelf-break surface flow and an eastward anomaly (strengthening) of the undercurrent, leading to increased ice-shelf melting. This contrasts with shorter time scales, for which surface current and undercurrent covary, a barotropic (depth-independent) behavior previously assumed to apply at all time scales. This suggests that interior ocean processes mediate the decadal ice-shelf response in the Amundsen Sea to climate forcing.

Plain Language Summary The West Antarctic Ice Sheet is losing mass, causing sea level rise. Most of this loss occurs in the Amundsen Sea Embayment, due to melting of coastal glaciers by warm ocean waters. These warm waters are transported toward the glaciers by the Amundsen Undercurrent, a near-seafloor eastward-flowing current located at the boundary between the deep ocean and the shallower seas around Antarctica. Changes in the undercurrent thus regulate the amount of heat available to melt the glaciers. Here, we use a model to assess the undercurrent's variability on time scales of decades, as decadal ocean forcing drives periods of enhanced ice-sheet retreat. Contrary to previous work, our model shows that wind fluctuations, associated with surface temperature changes in the tropical Pacific, lead to changes in the interior ocean density field on decadal time scales. Decadal anomalous cyclonic atmospheric circulation over the Amundsen Sea, associated with cooling in the tropical Pacific, accelerates the near-surface ocean flow westward, but also accelerates the eastward-flowing undercurrent and enhances glacial melting. Our work suggests that previous assumptions about the decadal oceanic response of the Amundsen Sea to wind variability might need to be reconsidered, with implications for melting of West Antarctic glaciers.

Key Points:

- Our modeled decadal strengthening of the Amundsen Undercurrent corresponds with increase in ice-shelf basal melting
- Undercurrent variability on decadal time scales is predominantly baroclinic (i.e., anticorrelated with the surface flow variability)
- At decadal timescales, this model shows enhanced ice-shelf melting under westward wind anomalies, a reverse relationship to previous studies

Supporting Information:

Supporting Information may be found in the online version of this article.

Correspondence to:

A. Silvano,
A.Silvano@soton.ac.uk

Citation:

Silvano, A., Holland, P. R., Naughten, K. A., Dragomir, O., Dutrieux, P., Jenkins, A., et al. (2022). Baroclinic ocean response to climate forcing regulates decadal variability of ice-shelf melting in the Amundsen Sea. *Geophysical Research Letters*, *49*, e2022GL100646. https://doi.org/10.1029/2022GL100646

Received 6 AUG 2022
Accepted 30 NOV 2022

Author Contributions:

Conceptualization: Alessandro Silvano, Paul R. Holland, Alberto C. Naveira Garabato
Formal analysis: Alessandro Silvano
Funding acquisition: Paul R. Holland, Adrian Jenkins, Alberto C. Naveira Garabato
Investigation: Alessandro Silvano
Methodology: Alessandro Silvano, Paul R. Holland, Kaitlin A. Naughten
Project Administration: Paul R. Holland
Software: Paul R. Holland, Kaitlin A. Naughten

1. Introduction

The Antarctic Ice Sheet is losing mass at an accelerating rate, contributing to global sea level rise (Rignot et al., 2019; Shepherd et al., 2018). The most rapid loss and retreat have been observed in the Amundsen Sea Embayment, West Antarctica, triggered by rapid ocean-driven melting of floating ice shelves in the eastern Amundsen Sea (Pritchard et al., 2012; Shepherd et al., 2004). Recent observational work has suggested that periods of enhanced West Antarctic Ice Sheet retreat are linked to decadal ocean variability (Jenkins et al., 2018), whereby warmer ocean conditions drive ice-shelf thinning, grounding line retreat, and ice-sheet mass loss.

Previous work (Jenkins et al., 2016) has linked the decadal variability of ocean properties on the eastern Amundsen Sea continental shelf to changes in the Amundsen Undercurrent that forms along the shelf break (Figure 1). The flow's structure at the shelf break (outside troughs) consists of a weak (mostly westward) cold (~freezing

Supervision: Paul R. Holland, Alberto C. Naveira Garabato
Validation: Alessandro Silvano, Paul R. Holland, Kaitlin A. Naughten, Oana Dragomir, Pierre Dutrieux, Adrian Jenkins, Yidongfang Si, Andrew L. Stewart, Beatriz Peña Molino, Gregor W. Janzing, Tiago S. Dotto, Alberto C. Naveira Garabato

temperature) flow near the surface and a strong, warm (>0°C) eastward current near the sea floor (the undercurrent; Walker et al., 2013, Figure 1b). The undercurrent transports warm and salty Circumpolar Deep Water. Multiple deep glacially incised troughs cross the continental shelf of the eastern Amundsen Sea, connecting the shelf break to the ice-shelf cavities. Once the undercurrent encounters these troughs, its flow is diverted onto the shelf and warm Circumpolar Deep Water can reach the base of the ice shelves (Figure 1a; Nakayama et al., 2013). When the Amundsen Undercurrent strengthens more ocean heat is advected onto the continental shelf (Dotto et al., 2019, 2020), ultimately increasing ice-shelf basal melting (Jenkins et al., 2016; Kimura et al., 2017).

The undercurrent variability has been linked to wind changes in the shelf-break region (Dotto et al., 2020; Wåhlin et al., 2013). At monthly time scales wind anomalies influence the barotropic (i.e., depth-independent) flow along the shelf break, implying that eastward (westward) anomalies of local winds cause undercurrent strengthening (weakening). In turn, wind anomalies at timescales up to interannual are correlated with observations of ocean heat content variations (Dutrieux et al., 2014; Kim et al., 2021) and ice-shelf thickness (Paolo et al., 2018). Based on these results, integrated wind anomalies at the shelf break of the eastern Amundsen Sea have been used as a proxy for the decadal variability in ocean heat on the shelf and glacial melting (Jenkins et al., 2016, 2018).

At interannual to decadal time scale, shelf-break winds in the Amundsen Sea are heavily influenced by tropical Pacific variability through atmospheric teleconnections (Holland et al., 2019; Li et al., 2021; Steig et al., 2012). Warmer sea surface temperature over the tropical Pacific (El Niño-like conditions) causes a weakening of the cyclonic atmospheric circulation in the Amundsen Sea (often referred to as the Amundsen Sea Low), resulting in eastward wind anomalies at the shelf break. Previous studies have focused on the barotropic response of the undercurrent to wind variability, suggesting enhanced ice-shelf melting under anti-cyclonic wind anomalies (Dotto et al., 2020; Dutrieux et al., 2014; Jenkins et al., 2016).

However, the baroclinic (i.e., depth-dependent) response remains unclear. Ocean pressure gradients (which induce geostrophic currents) are due to sea level gradients near the surface, but can be dominated by vertically integrated horizontal density gradients at greater depths. Thus, the vertical shear of the velocity at the shelf break is related to the density surfaces (i.e., isopycnals) sloping downward toward Antarctica (Figure 1b). This feature is known as the Antarctic Slope Front (Thompson et al., 2018). In this context, the undercurrent can be treated as a baroclinic current given that its presence is associated with the Antarctic Slope Front (Heywood et al., 1998; Walker et al., 2013). Here we consider a regional model of the Amundsen Sea to show that the undercurrent's barotropic response to atmospheric changes is dominant on short (less than 1 year) time scales, but that the baroclinic response (associated with the Antarctic Slope Front) determines the undercurrent's variability on decadal time scales. In our simulation, the baroclinic response opposes the barotropic response, resulting in increased ice-shelf melting in association with decadal-scale cyclonic atmospheric anomalies in the Amundsen Sea, contrary to previous assumptions.

2. Methods

2.1. Amundsen Sea Model

We analyze a hindcast simulation of the Amundsen Sea region using the MITgcm (Marshall et al., 1997) including components for the ocean, sea ice, and ice shelf. The model configuration is almost identical to the baseline simulation of Naughten et al. (2022) forced by ERA5 (Hersbach et al., 2020). The only difference is the treatment of iceberg meltwater, which here is injected uniformly around the coast, tapered linearly over a distance of 100 km offshore, spread evenly over the top 350 m of the ocean, and with a total flux of 100 Gt/yr. This change was found to make no significant difference to the simulation, and we therefore refer the reader to the full model description and validation of Naughten et al. (2022). The simulation period is 1979–2019, forced by the ERA5 atmospheric reanalysis, and it is preceded by a spin-up that repeats the first 24 years of the forcing. The lateral ocean boundaries are forced by a monthly climatology derived from observational products and state estimates (see Naughten et al., 2022), which therefore does not introduce additional decadal variability. This model has been shown to generally agree with the observed mean state and decadal variability, including warmer ocean conditions in the mid-late 2000s followed by cooling after 2010, even though the range of observed temperature variability is not perfectly captured by the model (Naughten et al., 2022). Because of the "forcing jump" applied to the model in 1979 we have removed from the analysis the first 5 years of the simulation, to allow for the baroclinic processes to fully develop. We also note that the model has a limitation because unrealistic cooling

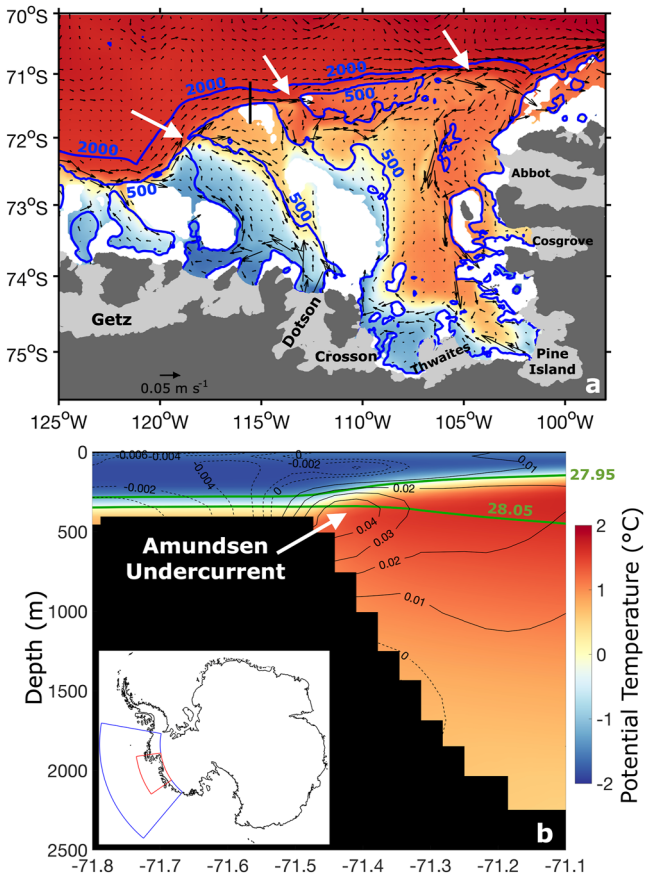

Figure 1. (a) Simulated time-mean (1984–2019) ocean potential temperature (°C, background color) and velocity (m s^{-1}, vectors) at 450 m depth in the Amundsen Sea. In blue are the 500- and 2,000-m isobaths (Morlighem et al., 2020). In white areas the sea floor is shallower than 450 m. Light gray regions indicate ice shelves, while grounded ice areas are in dark gray. White arrows highlight warm undercurrent intrusions onto the continental shelf along troughs. (b) Cross slope section (see black transect in (a) for location) of time-mean (1984–2019) potential temperature (°C, background color), along-slope velocity (m s^{-1}, dashed black contours for zero or negative values, solid black lines for positive values) and neutral density (kg m^{-3}, green; McDougall & Barker, 2011). Note the different contour spacing of negative and positive velocities. The inset highlights the model domain (blue) and the area shown in (a) (red).

occurs near the coast during a single event toward the end of the simulation (after 2013; Naughten et al., 2022). These cold anomalies are potentially due to a model bias that favors enhanced vertical mixing below the thermocline. This cooling event is localized near the coast and does not extend to the shelf break (Naughten et al., 2022), and therefore it is not expected to affect undercurrent variability, which is the focus of this work.

2.2. Climate Indices

To evaluate the role of tropical Pacific variability on decadal-scale atmospheric and oceanic changes in the Amundsen Sea, we consider the Tripole Index (TPI; https://www.esrl.noaa.gov/psd/data/timeseries/IPOTPI/) for the Interdecadal Pacific Oscillation (IPO). This index is based on the sea surface temperature anomaly in three areas of the Pacific Ocean (Henley et al., 2015). IPO variability has a broadly similar pattern to the El Niño-Southern Oscillation (ENSO) but acts on longer time scales. For this reason, the TPI is more appropriate in this study compared to other indices such as the Southern Oscillation Index, which is designed to describe interannual ENSO-related variability. Positive TPI values indicate warmer surface conditions in the tropical Pacific. We also consider the Southern Annular Mode (SAM) in the analysis, which captures the leading mode of atmospheric variability in the Southern Hemisphere. To first order, SAM describes changes of westerly winds over the entire Southern Ocean, whereby positive (negative) SAM is associated with strengthening (weakening) of the westerlies. The monthly SAM index is obtained from the British Antarctic Survey (G. Marshall, 2003; https://legacy.bas.ac.uk/met/gjma/sam.html). Monthly TPI and SAM indices are standardized before analysis.

2.3. Statistical Analysis

We perform correlation and coherence analyses of multiple ocean, atmospheric and climate variables. Anomalies are defined by removing the trend and seasonal cycle from each time series. Confidence levels for the cross correlations are estimated through a Student's *t*-test, taking into account the effective degrees of freedom for both monthly and 5-year smoothed time series. We consider time series smoothed with a 5-year running mean as representative of decadal variability (~10-year smoothing is typically used for investigating interdecadal variability; e.g., Henley et al., 2015). The number of effective degrees of freedom is obtained via the time scale over which the autocorrelation falls below 1/*e*. Correlations refer to 0-month lag, unless otherwise specified. Squared coherence quantifies the correlation between two time series in frequency space. Confidence levels are obtained following Equation 5.173 of Thomson and Emery (2014), after having applied a 7-year Hamming window to spectra and cross-spectra and no overlap.

3. Results

3.1. Baroclinic Undercurrent Variability on Decadal Time Scales

The modeled Amundsen Undercurrent pathway is defined for each longitudinal grid point by the latitude over the upper slope/shelf break (i.e., between the 500 and 1,500 m isobaths) where the time-mean along-slope flow in the Circumpolar Deep Water layer (neutral density > 27.95 kg m^{-3}) is maximum. The along-slope velocity is obtained by rotating the reference system to follow the 1,000 m isobath. We focus our attention on the eastern Amundsen Sea, between 125°W and 100°W. As we examine along shelf-break flow, and also to avoid contamination in the undercurrent signal by the complex trough dynamics (Saldías & Allen, 2020), we exclude the trough mouths from the definition of the undercurrent pathway (see Figure S1 in Supporting Information S1).

The undercurrent velocity is defined along the undercurrent pathway as the vertical average of the along-slope velocity between the depth of the 27.95 kg m^{-3} neutral density surface and the sea floor. Other definitions of the undercurrent velocity (e.g., maximum along-slope velocity in the vertical) do not affect the conclusions of this study, as confidence levels do not change.

Figure 2a shows velocity anomalies of undercurrent and surface geostrophic current (estimated from the cross-slope sea level gradient) spatially averaged along the undercurrent pathway. Hereafter we refer to the surface geostrophic current as surface current. This figure reveals that undercurrent and surface current are anti-correlated ($R = -0.84$, 95% significant) when a 5-year running mean is applied. A coherence analysis (Figure 2b) illustrates how this out-of-phase relationship emerges on decadal (~5 years) time scales (i.e., undercurrent and surface current are out of phase), while on monthly time scales the undercurrent variability is barotropic (i.e., undercurrent and surface current are in phase). At interannual time scales (~1–2 years) the coherence decreases. At decadal time scales we find no clear lag between undercurrent and surface flow (Figure 2b), suggesting that interior baroclinic adjustment occurs in less than 5 years and that the spatio-temporal smoothing procedure "filters out" the lag signal. This is also highlighted by the lag correlation between 5-year smoothed surface and undercurrent velocities (Figure S2 in Supporting Information S1), which shows a significant negative correlation at 0-month lag and a peak at 5-month lag. These results are consistent with those described in previous modeling works (Spence et al., 2014, 2017) showing how baroclinic changes of the flow at the shelf break (associated with the Antarctic Slope Front, see below) start to emerge less than a year after sea level changes.

Here we focus on the undercurrent over the entire eastern Amundsen Sea and therefore we spatially average the undercurrent velocities along the undercurrent pathway. The 5-year smoothed undercurrent velocities in different "sectors" of the shelf break (as defined in Figure S1 in Supporting Information S1) are highly correlated with one another ($R > 0.7$, 95% significant, see Figure S3a in Supporting Information S1). This indicates that spatial variability within the eastern Amundsen Sea does not affect the undercurrent's decadal variability as examined in this work.

3.2. Climate Forcing of Undercurrent's Decadal Variability

To better understand how the undercurrent responds to climate forcing at decadal time scales, we consider 5-year filtered time series from now on, unless otherwise specified. We estimate the correlation between surface flow/undercurrent and two climate indices: TPI and SAM. As suggested in previous work (Holland et al., 2019), we find a positive correlation between the TPI and the surface current at the shelf break ($R = 0.87$, 95% significant). Consistent with the anti-phased relationship described above, the undercurrent exhibits a negative correlation with the TPI ($R = -0.69$, 95% significant). We find no significant correlation between SAM and surface current or undercurrent, confirming how the non-annular atmospheric circulation regulated by tropical Pacific forcing determines decadal oceanic changes in the Amundsen Sea. While the correlation between undercurrent and TPI is relatively high, other mechanisms are likely to partly contribute to the undercurrent variability, including wind variability not captured by the TPI, local dynamical and thermodynamical feedbacks, and fluctuations of the Antarctic Circumpolar Current.

Now, to further investigate how the Amundsen Sea is influenced by tropical Pacific forcing, we average atmosphere and ocean properties during periods of negative TPI, corresponding to times of strengthened undercurrent (Figure 2a). We define times of negative TPI when the index is less than −0.37 (i.e., −1 standard deviation), noting that other thresholds (e.g., TPI < 0) do not affect the spatial patterns shown below. Opposite patterns to those described below occur during positive TPI (not shown). A negative period of the TPI (i.e., cooling in the tropical Pacific) is associated with a cyclonic atmospheric circulation anomaly centered near the northern boundary of the model domain, resulting in westward wind anomalies throughout the Amundsen Sea (Figures 3a and 3b). The ocean surface stress curl associated with this atmospheric pattern is positive on the continental shelf and negative further north (Figure 3b). This is due to the fact that the strongest westward wind anomalies occur at ~ 68–70°S, just north of the shelf break where the time-mean winds are westerlies (Figure 3a). Consequently, the curl of the wind field is positive to the south of the westerly wind band (Figure 3b). Through Ekman dynamics, this results in positive sea level anomalies on the continental shelf and negative anomalies off the shelf. This wind pattern drives (a) enhanced sea level near the coast relative to offshore (Figures 3c) and (b) deepening of the isopycnals on the continental shelf relative to offshore (where isopycnals do not show appreciable changes in depth; Figure 3d and Figure S4 in Supporting Information S1; see also Spence et al., 2014, 2017). Surface buoyancy forcing can also

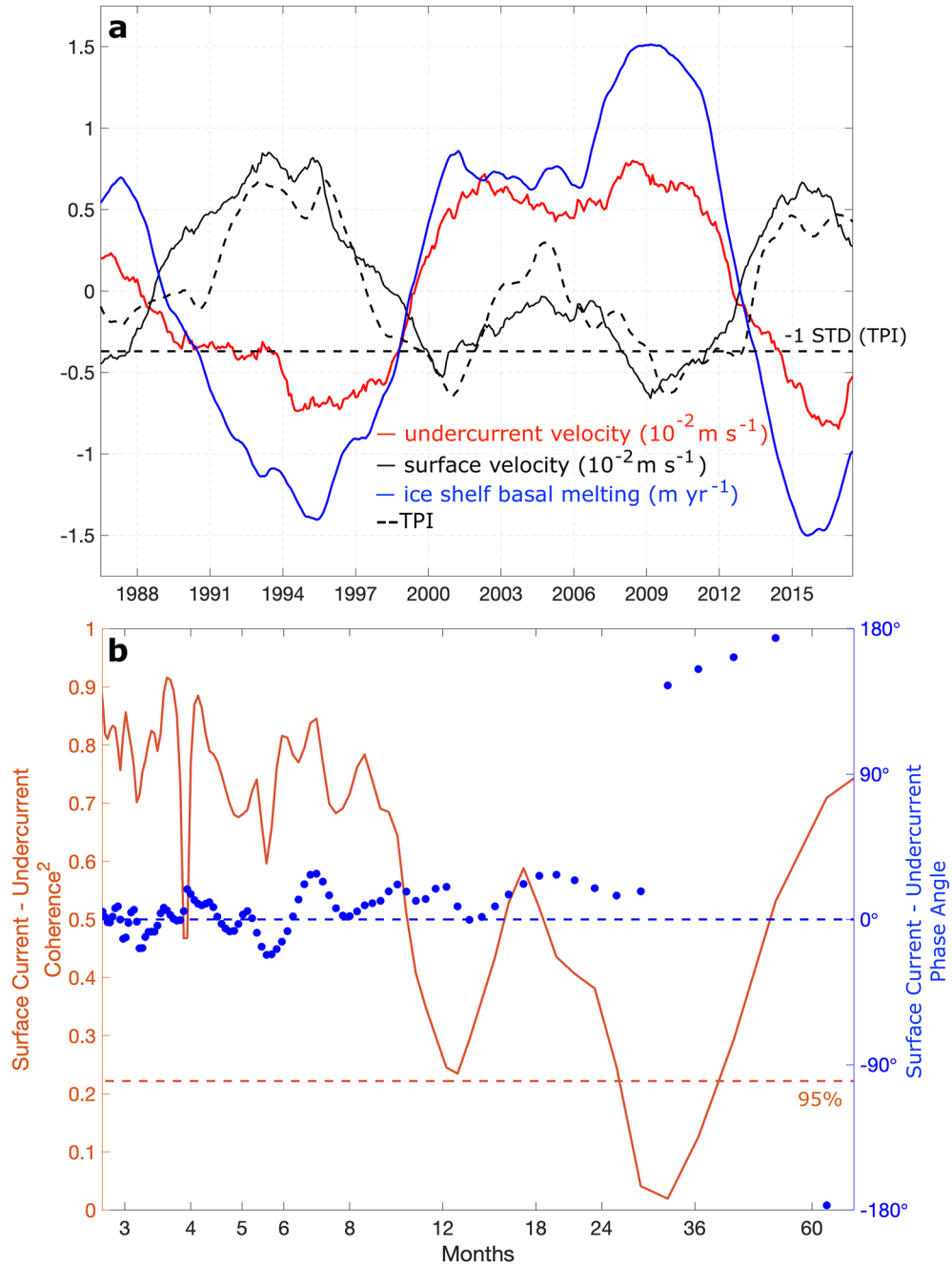

Figure 2. (a) Anomalies of undercurrent, surface current, Tripole Index (TPI) and spatially averaged basal melting of eastern Amundsen Sea ice shelves (i.e., Dotson, Crosson, Thwaites, Pine Island, and Cosgrove). We have removed the trend and seasonal cycle from each time series, and have applied a 5-year running mean. The legend shows color, scaling and unit associated with each time series. The horizontal dashed black line indicates the TPI value corresponding to −1 standard deviation (TPI = −0.37). All time series are correlated (95% significant) with each other, with TPI and surface current negatively correlated with undercurrent and ice-shelf basal melting. (b) Squared coherence (brown) and phase angle (blue) between surface current and undercurrent velocities. We have removed the trend and seasonal cycle from the time series, and no running mean has been applied before estimating the coherence. Note that a phase angle of ±180° at decadal time scales indicates that the two time series are out of phase, as the cross correlation between 5-year smoothed time series shows that at 30 months (half a period) lag/lead the correlation is not significant at 95% (see Figure S2 in Supporting Information S1). Highlighted in dashed brown is the 95% confidence level and in dashed blue is the 0° phase angle.

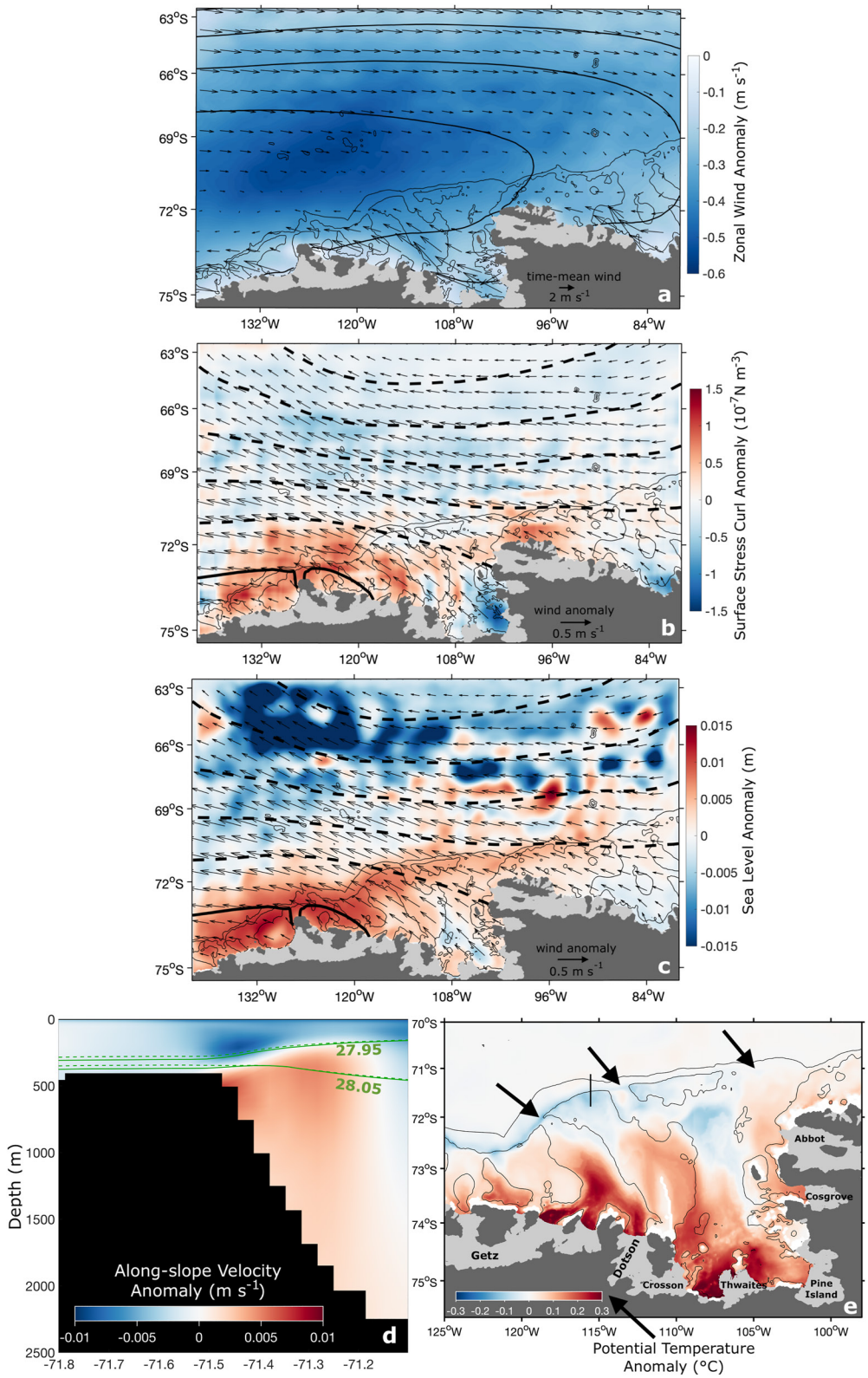
63°S
66°S
69°S
72°S
75°S
132°W
120°W
108°W
96°W
84°W
time-mean wind
2 m s-1
a
Zonal Wind Anomaly (m s-1)
0
-0.1
-0.2
-0.3
-0.4
-0.5
-0.6
wind anomaly
0.5 m s-1
b
Surface Stress Curl Anomaly (10-7N m-3)
1.5
1
0.5
0
-0.5
-1
-1.5
c
Sea Level Anomaly (m)
0.015
0.01
0.005
0
-0.005
-0.01
-0.015
Depth (m)
0
500
1000
1500
2000
2500
27.95
28.05
Along-slope Velocity
Anomaly (m s-1)
-0.01
-0.005
0
0.005
0.01
d
-71.8
-71.7
-71.6
-71.5
-71.4
-71.3
-71.2
70°S
71°S
72°S
73°S
74°S
75°S
Abbot
Cosgrove
Getz
Dotson
Crosson
Thwaites
Pine
Island
e
-0.3 -0.2 -0.1 0 0.1 0.2 0.3
125°W
120°W
115°W
110°W
105°W
100°W
Potential Temperature
Anomaly (°C)

Figure 3.

influence isopycnal depth on the continental shelf. However, we find that during negative TPI periods, surface fluxes act to cool and enhance salinity on the shelf (Figure S5 in Supporting Information S1) which, if relevant, would act to raise isopycnals by making waters denser (Stewart & Thompson, 2016), weakening the undercurrent. Finally, enhanced coastal sea level causes a sea-surface gradient anomaly that induces a westward flow anomaly near the surface at the shelf break, while steepening of the Antarctic Slope Front generates an eastward anomaly in (i.e., a strengthening of) the undercurrent (Figure 3d and Figure S4 in Supporting Information S1) through thermal wind balance. These results are consistent with a negative correlation ($R < -0.7$, 95% significant) between undercurrent and wind velocities in the westerly winds to the north of the shelf on decadal time scales (Figure S6b in Supporting Information S1), but contrast with monthly time scales. Indeed, at monthly time scales the undercurrent variability is barotropic and positively correlated with winds at the shelf break (Figure S6a in Supporting Information S1), as highlighted in previous works (Dotto et al., 2020; Wåhlin et al., 2013).

3.3. Climate Forcing of Decadal Ice-Shelf Melting in the Amundsen Sea

Our modeling work shows how the interior ocean adjustment to atmospheric forcing regulates the undercurrent strength on decadal time scales. Cyclonic wind anomalies during negative TPI periods are associated with undercurrent strengthening, coastal warming and enhanced ice-shelf basal melting (Figures 2a and 3e). However, the outer continental shelf exhibits a cooling signal. Cyclonic wind anomalies deepen the on-shelf isopycnals, causing the Antarctic Slope Front to steepen (Figure 3d), resulting in cooling near the shelf break in response to deepening of the thermocline (see Figure S7 in Supporting Information S1). In turn, undercurrent velocity changes regulate the temporal variability in ocean heat flux toward the coast (see Figure S8 in Supporting Information S1; Assmann et al., 2013; Kalen et al., 2016; Kimura et al., 2017; Wåhlin et al., 2013), and therefore this cooling signal disappears closer to the ice shelves. Local forcing on the continental shelf, such as surface buoyancy forcing (St-Laurent et al., 2015; Webber et al., 2017) and Ekman pumping (Donat-Magnin et al., 2017; Kim et al., 2021) affecting the depth of isotherms near the coast, can also contribute to changes in ice-shelf melting. While we cannot rule out that such processes may play a significant role, they are unlikely to be the main driver of decadal variability in this model (Kimura et al., 2017; see Supporting Information S1). The strong correlation ($R = 0.96$, 95% significant) between undercurrent velocity and ice-shelf basal melting further confirms that oceanic changes at the shelf break determine decadal variability in ice-shelf melting. If simulated years after 2013 (when the model exhibits unrealistic cooling near the coast, see Section 2) are not considered, the correlation between 5-year smoothed ice-shelf basal melt and undercurrent velocity remains strong (>0.9, 95% significant), consistent with the conclusion that undercurrent strength regulates ice-shelf basal melting at decadal time scales.

Note that we find virtually no lag between undercurrent velocity and ice-shelf basal melting on decadal time scales (i.e., the two time series are in phase; see Figure S9 in Supporting Information S1). This is consistent with the relatively short (few months) advective time between the shelf break and the ice-shelf cavities (Kimura et al., 2017), and with the spatio-temporal smoothing applied. We also estimate the modeled flushing time of the eastern Amundsen Sea continental shelf (i.e., continental shelf seawater volume divided by the volume flux onto the shelf; Text S2 in Supporting Information S1). We find that the flushing time is 18 ± 3 months, consistent with the residence time of Circumpolar Deep Water on the Amundsen Sea continental shelf estimated using simulated Lagrangian particle tracking (Tamsitt et al., 2021). This suggests that the continental shelf has a limited "buffering capacity" on time scales longer than interannual, consistent with the ice-shelf basal melting being directly related to the undercurrent velocity on decadal time scales.

Figure 3. (a) Time-mean (1984–2019) winds (vectors, m s^{-1}) and atmospheric surface pressure field (contours every 2 mbar) overlaid on zonal wind speed anomaly (background color) during negative Tripole Index (TPI). (b) Wind (vectors) and atmospheric pressure (contours every 0.25 mbar; dashed for negative and zero values, solid for positive values) anomalies overlaid on surface stress curl anomaly (background color, 10^{-7} N m^{-3}) during negative TPI. Here we have applied a 50-km spatial smoothing (rolling mean) to reduce noise arising from applying a spatial derivative to obtain the curl, but also because the surface stress curl is locally influenced by oceanic jet dynamics transferring momentum from the ocean to the sea ice (Stewart et al., 2019) that mask the large-scale forcing (see Figure S10 in Supporting Information S1). (c) Sea level anomaly (background color, m) during negative TPI. Vectors and contours as in (b). (d) Meridional section of along-slope velocity anomaly (m s^{-1}) during negative TPI. The transect location is highlighted in (e) by the thick black line. The solid green lines represent the 27.95 and 28.05 kg m^{-3} neutral density surfaces during negative TPI periods, while the dashed green lines indicate the time-mean (1984–2019) surfaces. (e) Map of potential temperature anomaly (°C) during negative TPI, vertically averaged between 200 m and the seafloor. The black arrows highlight where the undercurrent accesses the troughs. The 500- and 2,000-m isobaths are shown in all panels (except (d)) by the thin black lines.

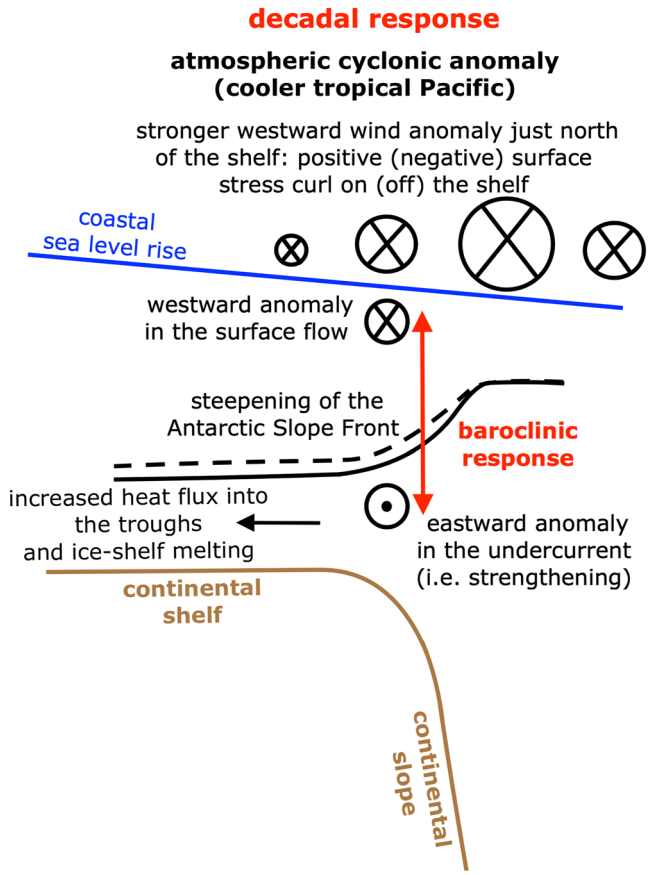

Figure 4. On decadal time scales the undercurrent variability is baroclinic and regulated by the surface stress curl. Anomalous atmospheric cyclonic circulation (cooler tropical Pacific) causes a westward wind anomaly throughout the Amundsen Sea, with the strongest anomaly occurring just north of the continental shelf. This results in positive anomalies of the surface stress curl on the continental shelf and negative off the shelf, driving sea level rise near the coast. This surface stress curl pattern is conducive to enhanced coastal sea level, causing westward anomalies of the surface flow; but it also acts to steepen the Antarctic Slope Front, generating an eastward anomaly (strengthening) of the undercurrent. Undercurrent strengthening ultimately drives enhanced ice-shelf basal melting.

4. Summary and Outlook

To summarize, our modeling work suggests a four-step process by which tropical Pacific variability regulates ice-shelf basal melting in the eastern Amundsen Sea on decadal time scales (Figure 4). (a) A cooler ocean surface in the tropical Pacific generates cyclonic wind anomalies in the Amundsen Sea. (b) Cyclonic wind anomalies and associated changes in the large-scale surface stress curl over the Amundsen Sea cause isopycnals to deepen on the continental shelf, resulting in Antarctic Slope Front steepening. (c) Steepening of the Antarctic Slope Front induces a baroclinic undercurrent strengthening. (d) Undercurrent strengthening causes on-shelf warming, increasing ice-shelf basal melting. The opposite happens during warmer tropical Pacific conditions. This view contrasts with the general assumption to date that the undercurrent weakens under cyclonic atmospheric anomalies when shelf-break winds exhibit westward anomalies (Dotto et al., 2020; Jenkins et al., 2016). This difference arises because previous work is founded on inferences from monthly to interannual variability, while our model indicates that an opposite response emerges at decadal time scales. Enhanced ice-shelf melting at decadal time scales can impact the ice sheet, as observed in the late 2000s with accelerated grounding line retreat and ice-sheet discharge in the eastern Amundsen Sea (Jenkins et al., 2018; Mouginot et al., 2014).

Our work suggests a key role for baroclinicity in influencing ocean decadal variability in the Amundsen Sea. However, this work relies on a single model which carries some limitations (see Methods). Other lines of evidence suggest that time-integrated barotropic anomalies of the undercurrent are important to decadal variability of ice-shelf melting (Jenkins et al., 2016). Moreover, both interannual (Dutrieux et al., 2014) and centennial (Naughten et al., 2022) ocean variability have been shown to affect ice-shelf melting, so the interplay between different frequencies of atmospheric forcing on ocean variability needs to be taken into account. Thus, more work is needed to investigate the role of baroclinic adjustment in the Amundsen Sea's in response to atmospheric forcing, potentially including simulations with more idealized settings and circumpolar domains (e.g., Verfaillie et al., 2022) as well as sustained long-term observations. Importantly, the regional model employed in this study is forced by monthly climatological boundary conditions, preventing assessment of the role of remote forcing, which has been shown to influence ocean temperatures on the Amundsen Sea continental shelf (Flexas et al., 2022; Nakayama et al., 2018). Finally, current climate models are too coarse to resolve oceanic processes on the Antarctic continental slope (Thompson et al., 2018). Our work highlights that increased resolution or improved parametrization of shelf-break processes are required in such models if they are to reliably predict future sea level rise due to melting of the West Antarctic Ice Sheet.

Data Availability Statement

The model output is publicly accessible (Silvano & Holland, 2022).

Acknowledgments
The authors thank two anonymous reviewers for their constructive comments, which greatly helped to improve this manuscript. This research is part of the UKRI-JSPS project "Quantifying Human Influence on Ocean Melting of the West Antarctic Ice Sheet" NE/S011994/1. A.S. acknowledges funding from NERC (NE/V014285/1).

References

Assmann, K. M., Jenkins, A., Shoosmith, D. R., Walker, D. P., Jacobs, S. S., & Nicholls, K. W. (2013). Variability of Circumpolar Deep Water transport onto the Amundsen Sea continental shelf through a shelf break trough. *Journal of Geophysical Research: Oceans*, *118*(12), 6603–6620. https://doi.org/10.1002/2013JC008871

Donat-Magnin, M., Jourdain, N. C., Spence, P., Le Sommer, J., Gallée, H., & Durand, G. (2017). Ice-shelf melt response to changing winds and glacier dynamics in the Amundsen Sea Sector, Antarctica. *Journal of Geophysical Research: Oceans*, *122*(12), 10206–10224. https://doi.org/10.1002/2017JC013059

Dotto, T. S., Naveira Garabato, A. C., Bacon, S., Holland, P. R., Kimura, S., Firing, Y. L., et al. (2019). Wind-driven processes controlling oceanic heat delivery to the Amundsen Sea, Antarctica. *Journal of Physical Oceanography*, *49*(11), 2829–2849. https://doi.org/10.1175/JPO-D-19-0064.1

Dotto, T. S., Naveira Garabato, A. C., Wåhlin, A. K., Bacon, S., Holland, P. R., Kimura, S., et al. (2020). Control of the oceanic heat content of the Getz-Dotson trough, Antarctica, by the Amundsen Sea Low. *Journal of Geophysical Research: Oceans*, *125*(8), e2020JC016113. https://doi.org/10.1029/2020JC016113

Dutrieux, P., De Rydt, J., Jenkins, A., Holland, P. R., Ha, H. K., Lee, S. H., et al. (2014). Strong sensitivity of Pine Island ice-shelf melting to climatic variability. *Science*, *343*(6167), 174–178. https://doi.org/10.1126/science.1244341

Flexas, M. M., Thompson, A. F., Schodlok, M. P., Zhang, H., & Speer, K. (2022). Antarctic Peninsula warming triggers enhanced basal melt rates throughout West Antarctica. *Science Advances*, *8*(31), eabj9134. https://doi.org/10.1126/sciadv.abj9134

Henley, B., Gergis, J., Karoly, D., Power, S., Kennedy, J., & Folland, C. (2015). A tripole index for the Interdecadal Pacific Oscillation. *Climate Dynamics*, *45*(11–12), 3077–3090. https://doi.org/10.1007/s00382-015-2525-1

Hersbach, H., Bell, B., Berrisford, P., Hirahara, S., Horányi, A., Muñoz-Sabater, J., et al. (2020). The ERA5 global reanalysis. *Quarterly Journal of the Royal Meteorological Society*, *146*(730), 1999–2049. https://doi.org/10.1002/qj.3803

Heywood, K. J., Locarnini, R. A., Frew, R. D., Dennis, P. F., & King, B. A. (1998). Transport and water masses of the Antarctic Slope Front System in the Eastern Weddell Sea. In S. S. Jacobs & R. F. Weiss (Eds.), *Ocean, ice, and atmosphere: Interactions at the Antartic continental margin*, *Antarctic research series* (Vol. 75, pp. 203–214). American Geophysical Union.

Holland, P. R., Bracegirdle, T. J., Dutrieux, P., Jenkins, A., & Steig, E. J. (2019). West Antarctic ice loss influenced by internal climate variability and anthropogenic forcing. *Nature Geoscience*, *12*(9), 718–724. https://doi.org/10.1038/s41561-019-0420-9

Jenkins, A., Dutrieux, P., Jacobs, S. S., Steig, E. J., Gudmundsson, G. H., Smith, J., & Heywood, K. J. (2016). Decadal ocean forcing and Antarctic ice sheet response: Lessons from the Amundsen Sea. *Oceanography*, *29*(4), 106–117. https://doi.org/10.5670/oceanog.2016.103

Jenkins, A., Shoosmith, D., Dutrieux, P., Jacobs, S., Kim, T. W., Lee, S. H., & Stammerjohn, S. (2018). West Antarctic Ice Sheet retreat in the Amundsen Sea driven by decadal oceanic variability. *Nature Geoscience*, *11*(10), 733–738. https://doi.org/10.1038/s41561-018-0207-4

Kalén, O., Assmann, K. M., Wåhlin, A. K., Ha, H. K., Kim, T. W., & Lee, S. H. (2016). Is the oceanic heat flux on the central Amundsen Sea shelf caused by barotropic or baroclinic currents? *Deep Sea Research Part II*, *123*, 7–15. https://doi.org/10.1016/j.dsr2.2015.07.014

Kim, T.-W., Yang, H. W., Dutrieux, P., Wåhlin, A. K., Jenkins, A., Kim, Y. G., et al. (2021). Interannual variation of modified circumpolar deep water in the Dotson-Getz Trough, West Antarctica. *Journal of Geophysical Research: Oceans*, *126*(12), e2021JC017491. https://doi.org/10.1029/2021JC017491

Kimura, S., Jenkins, A., Regan, H., Holland, P. R., Assmann, K. M., Whitt, D. B., et al. (2017). Oceanographic controls on the variability of ice-shelf basal melting and circulation of glacial meltwater in the Amundsen Sea Embayment, Antarctica. *Journal of Geophysical Research: Oceans*, *122*(12), 10131–10155. https://doi.org/10.1002/2017JC012926

Li, X., Cai, W., Meehl, G. A., Chen, D., Yuan, X., Raphael, M., et al. (2021). Tropical teleconnection impacts on Antarctic climate changes. *Nature Reviews Earth & Environment*, *2*(10), 680–698. https://doi.org/10.1038/s43017-021-00204-5

Marshall, G. (2003). Trends in the Southern Annular Mode from observations and reanalyses. *Journal of Climate*, *16*(24), 4134–4143. https://doi.org/10.1175/1520-0442(2003)016<4134:TITSAM>2.0.CO;2

Marshall, J., Hill, C., Perelman, L., & Adcroft, A. (1997). Hydrostatic, quasi-hydrostatic, and nonhydrostatic ocean modeling. *Journal of Geophysical Research*, *102*(C3), 5733–5752. https://doi.org/10.1029/96JC02776

McDougall, T. J., & Barker, P. M. (2011). Getting started with TEOS-10 and the Gibbs seawater (GSW) Oceanographic Toolbox. SCOR/IAPSO WG127. (p. 28). 978-0-646-55621-5.

Morlighem, M., Rignot, E., Binder, T., Blankenship, D., Drews, R., Eagles, G., et al. (2020). Deep glacial troughs and stabilizing ridges unveiled beneath the margins of the Antarctic Ice Sheet. *Nature Geoscience*, *13*(2), 132–137. https://doi.org/10.1038/s41561-019-0510-8

Mouginot, J., Rignot, E., & Scheuchl, B. (2014). Sustained increase in ice discharge from the Amundsen Sea Embayment, West Antarctica, from 1973 to 2013. *Geophysical Research Letters*, *41*(5), 1576–1584. https://doi.org/10.1002/2013GL059069

Nakayama, Y., Menemenlis, D., Zhang, H., Schodlok, M., & Rignot, E. (2018). Origin of circumpolar deep water intruding onto the Amundsen and Bellingshausen Sea continental shelves. *Nature Communications*, *9*(1), 3403. https://doi.org/10.1038/s41467-018-05813-1

Nakayama, Y., Schröder, M., & Hellmer, H. H. (2013). From circumpolar deep water to the glacial meltwater plume on the eastern Amundsen Shelf. *Deep-Sea Research I*, *77*, 50–62. https://doi.org/10.1016/j.dsr.2013.04.001

Naughten, K. A., Holland, P. R., Dutrieux, P., Kimura, S., Bett, D. T., & Jenkins, A. (2022). Simulated twentieth-century ocean warming in the Amundsen Sea, West Antarctica. *Geophysical Research Letters*, *49*(5), e2021GL094566. https://doi.org/10.1029/2021GL094566

Paolo, F. S., Padman, L., Fricker, H. A., Adusumilli, S., Howard, S., & Siegfried, M. R. (2018). Response of Pacific-sector Antarctic ice shelves to the El Niño/Southern Oscillation. *Nature Geoscience*, *11*(2), 121–126. https://doi.org/10.1038/s41561-017-0033-0

Pritchard, H. D., Ligtenberg, S. R. M., Fricker, H. A., Vaughan, D. G., van den Broeke, M. R., & Padman, L. (2012). Antarctic ice–sheet loss driven by basal melting of ice shelves. *Nature*, *484*(7395), 502–505. https://doi.org/10.1038/nature10968

Rignot, E., Mouginot, J., Scheuchl, B., Van Den Broeke, M., Van Wessem, M. J., & Morlighem, M. (2019). Four decades of Antarctic Ice Sheet mass balance from 1979–2017. *Proceedings of the National Academy of Sciences*, *116*(4), 1095–1103. https://doi.org/10.1073/pnas.1812883116

Saldías, G. S., & Allen, S. E. (2020). The influence of a submarine canyon on the circulation and cross-shore exchanges around an upwelling front. *Journal of Physical Oceanography*, *50*(6), 1677–1698. https://doi.org/10.1175/jpo-d-19-0130.1

Shepherd, A., Ivins, E., Rignot, E., Smith, B., van den Broeke, M., Velicogna, I., et al. (2018). Mass balance of the Antarctic ice sheet from 1992 to 2017. *Nature*, *558*, 219–222. https://doi.org/10.1038/s41586-018-0179-y

Shepherd, A., Wingham, D., & Rignot, E. (2004). Warm ocean is eroding West Antarctic Ice Sheet. *Geophysical Research Letters*, *31*(23), L23402. https://doi.org/10.1029/2004GL021106

Silvano, A., & Holland, P. H. (2022). Baroclinic ocean response to climate forcing regulates decadal variability in ice-shelf melting. https://doi.org/10.5281/zenodo.6940863

Spence, P., Griffies, S. M., England, M. H., Hogg, A. M., Saenko, O. A., & Jourdain, N. C. (2014). Rapid subsurface warming and circulation changes of Antarctic coastal waters by poleward shifting winds. *Geophysical Research Letters*, *41*(13), 4601–4610. https://doi.org/10.1002/2014gl060613

Spence, P., Holmes, R. M., Hogg, A. M., Griffies, S. M., Stewart, K. D., & England, M. H. (2017). Localized rapid warming of West Antarctic subsurface waters by remote winds. *Nature Climate Change*, *7*(8), 595–603. https://doi.org/10.1038/nclimate3335

Steig, E. J., Ding, Q., Battisti, D. S., & Jenkins, A. (2012). Tropical forcing of circumpolar deep water inflow and outlet glacier thinning in the Amundsen Sea Embayment, West Antarctica. *Annals of Glaciology*, *53*(60), 19–28. https://doi.org/10.3189/2012AoG60A110

Stewart, A. L., Klocker, A., & Menemenlis, D. (2019). Acceleration and overturning of the Antarctic Slope Current by winds, eddies, and tides. *Journal of Physical Oceanography*, *49*(8), 2043–2074. https://doi.org/10.1175/jpo-d-18-0221.1

Stewart, A. L., & Thompson, A. F. (2016). Eddy generation and jet formation via dense water outflows across the Antarctic continental slope. *Journal of Physical Oceanography*, *46*(12), 3729–3750. https://doi.org/10.1175/JPO-D-16-0145.1

St-Laurent, P., Klinck, J. M., & Dinniman, M. S. (2015). Impact of local winter cooling on the melt of Pine Island Glacier, Antarctica. *Journal of Geophysical Research: Oceans*, *120*(10), 6718–6732. https://doi.org/10.1002/2015JC010709

Tamsitt, V., England, M. H., Rintoul, S. R., & Morrison, A. K. (2021). Residence time and transformation of warm Circumpolar Deep Water on the Antarctic continental shelf. *Geophysical Research Letters*, *48*(20), e2021GL096092. https://doi.org/10.1029/2021GL096092

Thompson, A. F., Stewart, A. L., Spence, P., & Heywood, K. J. (2018). The Antarctic Slope Current in a changing climate. *Reviews of Geophysics*, *56*(4), 741–770. https://doi.org/10.1029/2018RG000624

Thomson, W. J., & Emery, R. E. (2014). *Data analysis methods in Physical Oceanography* (3rd ed.). Elsevier Science.728.

Verfaillie, D., Pelletier, C., Goosse, H., Jourdain, N. C., Bull, C. Y. S., Dalaiden, Q., et al. (2022). The circum-Antarctic ice-shelves respond to a more positive Southern Annular Mode with regionally varied melting. *Communications Earth & Environment*, *3*(1), 139. https://doi.org/10.1038/s43247-022-00458-x

Walker, D. P., Jenkins, A., Assmann, K. M., Shoosmith, D. R., & Brandon, M. A. (2013). Oceanographic observations at the shelf break of the Amundsen Sea, Antarctica. *Journal of Geophysical Research: Oceans*, *118*(6), 2906–2918. https://doi.org/10.1002/jgrc.20212

Wåhlin, A. K., Kalén, O., Arneborg, L., Björk, G., Carvajal, G. K., Ha, H. K., et al. (2013). Variability of warm deep water inflow in a sub-marine trough on the Amundsen Sea shelf. *Journal of Physical Oceanography*, *43*(10), 2054–2070. https://doi.org/10.1175/JPO-D-12-0157.1

Webber, B. G., Heywood, K. J., Stevens, D. P., Dutrieux, P., Abrahamsen, E. P., Jenkins, A., et al. (2017). Mechanisms driving variability in the ocean forcing of Pine Island Glacier. *Nature Communications*, *8*(1), 14507. https://doi.org/10.1038/ncomms14507